IEEE Photonics Journal
An IEEE Photonics Society Publication

Open Access

Sol–Gel Synthesis of Au/Cu-TiO_2 Nanocomposite and Their Morphological and Optical Properties

Volume 5, Number 3, June 2013

M. A. Gondal
S. G. Rashid
M. A. Dastageer
S. M. Zubair
M. A. Ali
J. H. Lienhard
G. H. McKinley
K. K. Varanasi

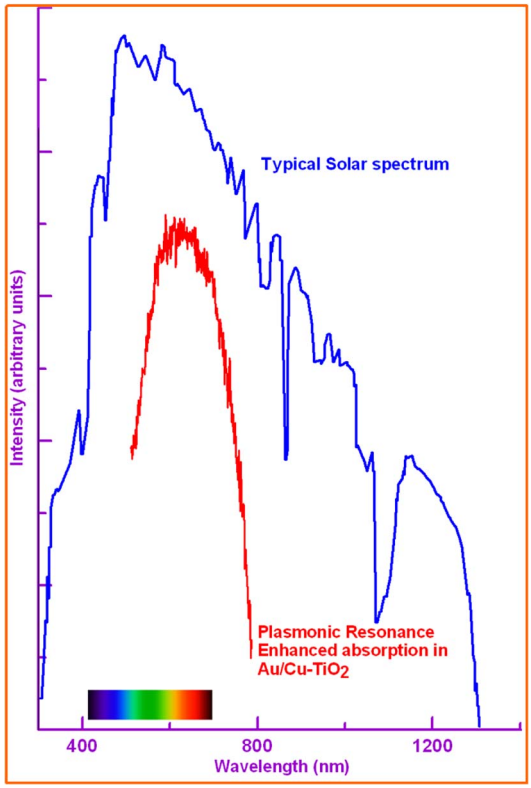

DOI: 10.1109/JPHOT.2013.2262674
1943-0655/$31.00 ©2013 IEEE

IEEE photonics SOCIETY

IEEE

Sol–Gel Synthesis of Au/Cu-TiO_2 Nanocomposite and Their Morphological and Optical Properties

M. A. Gondal,[1] S. G. Rashid,[1] M. A. Dastageer,[1] S. M. Zubair,[2] M. A. Ali,[3] J. H. Lienhard,[4] G. H. McKinley,[4] and K. K. Varanasi[4]

[1]Department of Physics and Center of Excellence in Nanotechnology (CENT), King Fahd University of Petroleum and Minerals (KFUPM), Dhahran 31261, Saudi Arabia
[2]Mechanical Engineering Department, KFUPM, Dhahran 31261, Saudi Arabia
[3]Center for Refining and Petrochemicals, Research Institute, KFUPM, Dhahran 31261, Saudi Arabia
[4]Mechanical Engineering Department, Massachusetts Institute of Technology, Cambridge, MA 02139-4307 USA

DOI: 10.1109/JPHOT.2013.2262674

Manuscript received April 16, 2013; revised May 4, 2013; accepted May 6, 2013. Date of current version June 20, 2013. This work was supported by KFUPM and MIT under Projects MIT11109 and MIT11110.
Corresponding author: M. A. Gondal (e-mail: magondal@kfupm.edu.sa).

Abstract: A facile single-step method was adopted to synthesize gold-modified copper-doped titania nanocomposites. Physicochemical properties of the synthesized material were characterized by X-ray diffraction (XRD), diffuse reflectance spectroscopy, photoluminescence (PL), and TEM-based techniques. Our characterizations show that the material consisted of anatase-phase qausi-spherical titania nanoparticles (NPs), with 3–4-nm gold particles anchored on titania surface. According to diffuse UV-visible spectroscopic analysis, gold-modified copper-doped titania shows enhanced absorption in the visible-light spectrum compared with copper-doped titania and pure titania. Furthermore, a decrease in PL emission intensity is observed, and this is due to decreased electron–hole recombination, which is an attribute desired for the enhancement of photocatalytic activity. Our present results highlight that these nanocomposites could be used as a photocatalyst for various applications in conjunction with visible solar radiation. The surface modifications make this material for many applications such as gas sensing and photodetection.

Index Terms: Titania-based nanocomposites, sol–gel technique, gold modification, photoluminescence (PL).

1. Introduction

Titania (TiO_2) has been on the spotlight of intense research for the past few decades due to its chemical, economic, and environmental merits. However, its inefficiency in utilizing solar energy coupled with low quantum efficiency and poor photocatalytic activity restricts the potential of this material. Since the pioneer work of Fujishima and Honda [1], various modifications [2] have been developed to extend spectral response in the visible-light spectrum, increase mobility of charges, and enhance photocatalytic activity of titania. Titania doped with copper has been successfully used for the effective photoreduction of carbon dioxide [3], [4], better photocatalytic degradation [5], hydrogen production [6], and improved gas sensing properties [7]. In addition to photocatalytic application, the TiO_2 nano/microsphere array [8]–[10] deposited via a rapid convective deposition method [11], [12] had been recently pursued for achieving improved light extraction efficiency in III-Nitride LEDs due to its index matching to GaN platform [8], [9].

In addition, the visible light active Cu_xO/TiO_2 is the focus of research as a risk reduction material for indoor environment [13]. However, copper-doped titania is more photocorrosive compared with titania. When metals are used as dopants, they should be resistant to the photo oxidation process for getting stable and durable materials. In order to have such good attributes of doping with metals, noble metals in general and gold in particular are quite appropriate to make modification to titania [14], [15]. As gold has the capacity to produce the highest Schottky barrier [14] like platinum, it can avoid the electron–hole recombination process, by assisting in electron capture. In addition to this, the optical properties of the gold-modified titania are enhanced due to surface plasmon resonance. Plasmonic photocatalysis is receiving a lot of attention because of excellent mobility of charge carriers, increased path length of light in the plasmonic structure due to efficient scattering enhanced rate of electron–hole formation at the surface of the semiconductor in the proximity of the plasmonic structure, super linear power law dependence at significantly low intensity, and enhancement in the photocatalytic efficiencies with operating temperature [16]–[18].

The metal oxide has a very pronounced surface effect, and hence, the optical properties could be changed by engineering the surface effect, and this has attracted many research efforts for versatile applications such as memory, transistors, light emission, gas sensing, and photodetection. The recent works of Chen *et al.* showed that the surface effect can be generic to all nanostructures and have quantitatively shown that surface band bending of ZnO nanowires is 1.54 eV with the width of 43.2 nm [19], [20]. Moreover, the modification of Au nanoparticles (NPs) on the surfaces of an n-type metal oxide nanostructure can create nano-Schottky junctions and enhances the formation of the charge O_2 adsorbates, causing the unusually high surface band bending of 2.34 eV with a wide width of 53.3 nm and also the tunability of optical emission [21], [22]. It was also observed that in an Al_2O_3 nanocrystal coating layer, leading to a flatband effect near the ZnO surface, causing a stronger overlap of the wavefunctions of electrons and holes in the ZnO core, and this effect leads to the enhancement of the near-band-edge emission [23].

In this paper, the synthesis of gold-modified copper-doped titania $(Au/Cu\text{-}TiO_2)$ at a very low concentration is carried out, and the effect of modification on the optical and structural properties of the modified titania matrix is investigated for some possible applications where solar energy can be effectively utilized. Moreover, the relative merits of pure titania (TiO_2), copper-doped titania $(Cu\text{-}TiO_2)$, and gold-modified copper-doped titania $(Au/Cu\text{-}TiO_2)$ in terms of their properties and applications have been studied. It was observed in our work that $Au/Cu\text{-}TiO_2$ exhibited a considerable absorption in the visible region. This property of enhanced quantum yield in the visible region shows this material as a suitable candidate for photocatalytic applications in the visible region. One of the major research areas of interest is the need for material for sensing applications, and as $Au/Cu\text{-}TiO_2$ shows an enhanced photo activity and quantum efficiency in the visible region, it can be a good candidate for sensing applications such as detection of heavy metals like arsenic, chromium, lead, mercury, etc. in water bodies.

2. Experimental

2.1. Catalyst Synthesis

The flowchart diagram shown in Fig. 1 shows the synthesis scheme for TiO_2, $Cu\text{-}TiO_2$, and $Au/Cu\text{-}TiO_2$ by a single-step modified sol–gel method. During this process, a solution of an appropriate amount of urea is mixed with 0.043 g of gold (III) chloride (Aldrich, 99.9%) and copper (II) nitrate (Aldrich, 99.9%), and this mixture is added to a solvent mixture of water, anhydrous ethanol (Aldrich, 99.5%), and acetic acid (Aldrich, 99.7%) in a 1 : 7 : 2 ratio by volume at 10 °C. 118.5 ml of titanium isopropoxide (TTIP) (Aldrich, 97%) was added into this solution dropwise, and the solution was kept in the dark room for 24 h with vigorous stirring for the nucleation process. After 24 h, the aging and gelation process was initiated by placing this solution in an oven at 70 °C for 6 h. This material (dry gel) was pulverized into powder and calcined

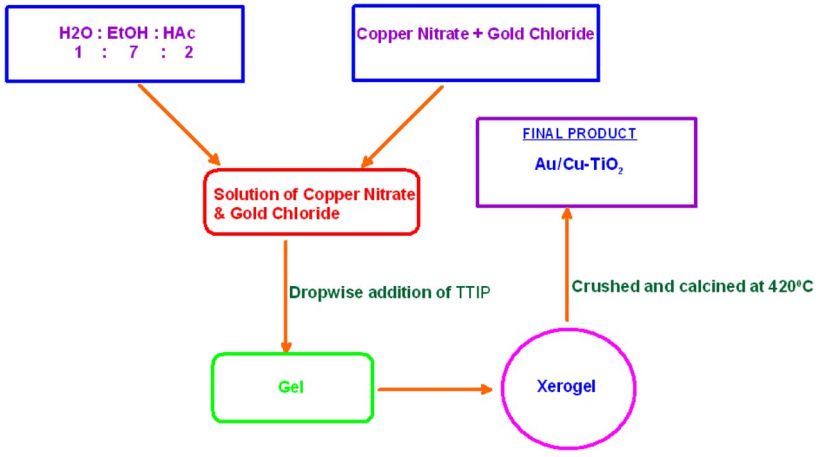

Fig. 1. The synthesis method of Au/Cu-TiO_2 nanocomposites.

for 3 h at 420 °C in a tube furnace. A similar methodology was adopted for the synthesis of TiO_2, Cu-TiO_2 NPs.

2.2. Material Characterization

X-ray diffraction (XRD) patterns of the synthesized nanomaterials were recorded in the range of 2θ between 10° and 80° with a step size of 0.02 and scan speed of 2 deg/min on a Philips X'Pert MPD rotatory target diffractometer, using CuKα radiation $(= 0.15406\ \text{nm})$ as an X-ray source, operated at 40 kV and 30 mA. Transmission electron microscopy (TEM) of Cu-TiO_2 as well as Au/Cu-TiO_2 was carried out using high-resolution TEM (HRTEM) (FEI model TitanG2 80-300 TEM). This transmission electron microscope was also equipped with an X-ray energy-dispersive spectroscope (EDS) detector and a high-angle annular dark-field (HAADF) detector for elemental and scanning TEM (STEM) analyses, respectively. The entire analysis was performed by operating the HRTEM at 300 keV to achieve the best line resolution in the acquired HRTEM as well as in the STEM mode. HRTEM micrographs of the samples were acquired with a 4000 $\times$ 4000 pixels charged-coupled device (CCD) camera (Gatan, Inc. model US 4000), and the acquired micrographs were processed in Gatan's Digital Micrograph Software Suite. The microscope magnification of around one-half million was set before the acquisition of HRTEM images while a magnification of one million was used to acquire STEM images. Fast Fourier transform (FFT) analysis was also performed on the acquired HRTEM micrographs in order to measure the d-spacings of the TiO_2 phase. The optical absorption spectrum of the synthesized material was carried out with the spectrophotometer (Jasco 670), with an appropriate baseline. The photoluminescence (PL) spectrum of the sample was carried out with the spectrofluorophotometer (Shimadzu RF- 5301PC) equipped with a grating of 1200-g/mm groove density, and the 150-W xenon lamp kept at a 325-nm wavelength is the excitation source.

3. Results and Discussion

3.1. Crystal Structure and Morphology

Fig. 2 shows the XRD patterns of TiO_2, Cu-TiO_2, and Au/Cu-TiO_2. The XRD patterns in Fig. 2 is the typical one for the anatase TiO_2 with no presence of extra phase of impurity but clearly showing the dopants dispersed homogeneously on the titania matrix. The copper doping in the titania matrix makes the XRD peaks to being slightly shifted toward left, although the shifting is not quite prominent. This shift of the XRD peaks is less prominent because the ionic radius of Cu^{2+} (0.72 Å) is slightly bigger than that of Ti^{4+} (0.68 Å) that produce strain in the titania lattice. The HRTEM image of Cu-TiO_2 in Fig. 3(a) shows an enhancement in d-spacing of 101 planes. For the pure

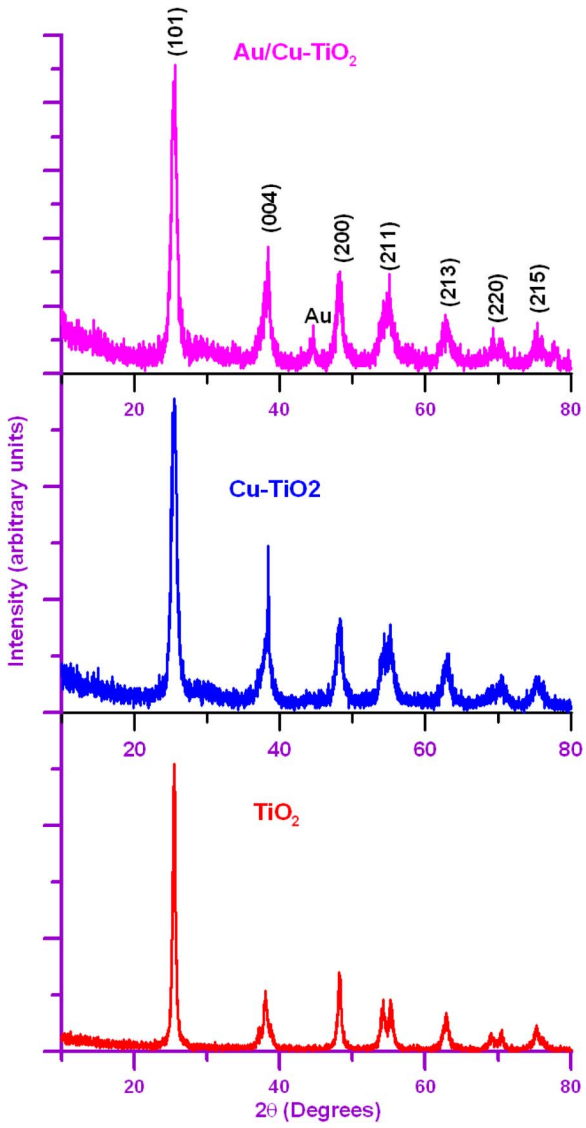

Fig. 2. XRD patterns TiO_2, Cu-TiO_2, and Au/Cu-TiO_2. HRTEM image of Cu-TiO_2 in the inset shows the d-spacing.

anatase TiO_2, it was estimated that the d-spacing value of the 101 planes is 0.351 nm, and that for the copper-doped TiO_2 is 0.358 nm, which confirms the slight left shift of the 101 planes of Cu-TiO_2 observed in our work. Moreover, the d-spacing of 101 planes measured from XRD data is 0.357 nm for Cu-TiO_2. In a recent detailed study of Cu-TiO_2 [24], X-ray absorption near edge structure (XANES) and extended X-ray absorption fine structure (EXAFS) and total scattering and pair distribution function (PDF) analysis with different fitting models, it was concluded that copper remained as a surface dopant, mostly as oxide or hydroxide phase on the surface of TiO_2. In the same study, one of the fitting models of total scattering PDF suggested that copper is substituted at the titanium site with oxygen vacancies. However, due to low concentration of dopant and in order to complement EXAFS data, this explanation was not considered. In our study, the enhanced d-spacing of 101 planes of Cu-TiO_2, as shown in the HRTEM image, suggests that some amount of copper is substituted in titanium sites. Hence, in the light of the above two studies, one may conclude that some amount of copper remained at the surface of TiO_2 and some substitute Ti^{+4}. Moreover, in the XRD analysis, broadening of TiO_2 peaks with copper doping favored the

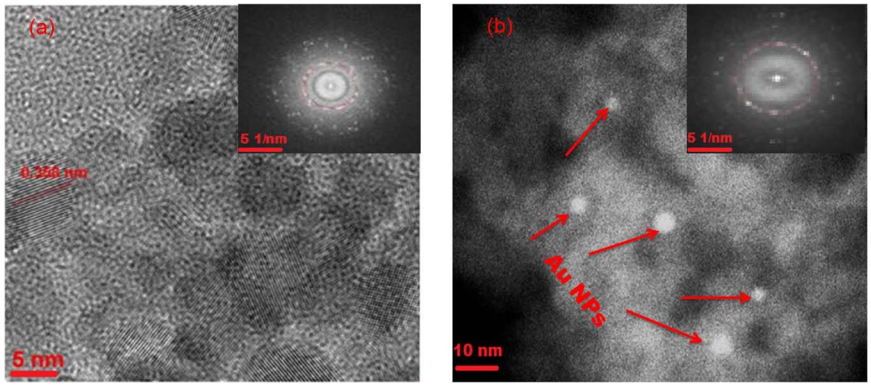

Fig. 3. (a) HRTEM micrograph of Cu-TiO_2 and (b) HAADF-STEM micrograph of Au/Cu-TiO_2, both with FFT as an inset.

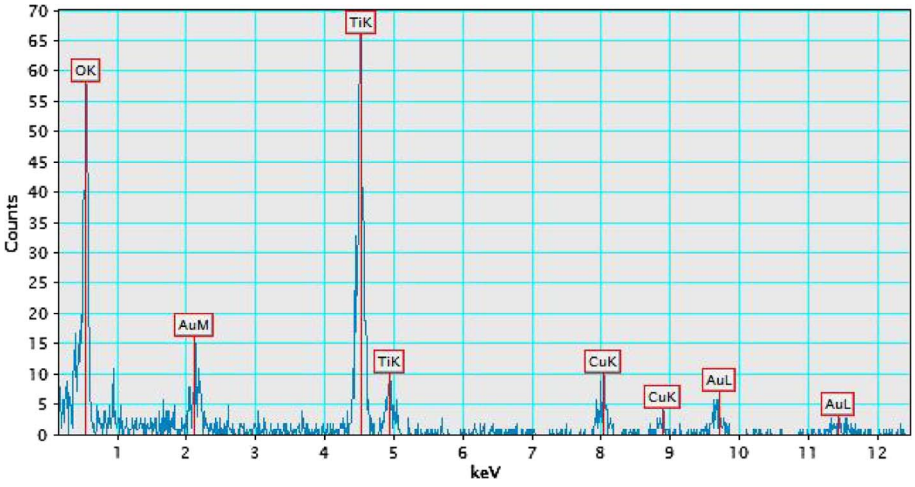

Fig. 4. EDX spectrum of Au/Cu-TiO_2.

substitution of Cu^{+2} at Ti^{+4} sites. After gold modification on Cu-TiO_2, no further shift is observed in d-spacing because the ionic radius of gold ($Au^{+3} = 0.99$ Å) [25] is much larger than Ti^{4+}. Hence, it is assumed that gold is adsorbed on the titania crystallites due to surface interaction.

The HRTEM micrograph of Cu-TiO_2 [see Fig. 3(a)], along with its FFT that is shown as an inset in the micrograph, is showing the typical size and shape of copper-doped titania NPs. The HAADF-STEM technique is very sensitive to the atomic number of elements and generally possesses a high composition contrast in the acquired images. In our case, as Au and Ti have a large difference in their atomic numbers, it is possible to detect even a small amount of Au in the Cu-TiO_2 samples. In addition to this, HAADF or Z-contrast images shed light on the structural changes in the sample at the nano level. As an example of it, a typical HAADF-STEM micrograph, along with FFT as an inset, is shown in Fig. 3(b). It clearly depicts the presence of 4-nm or smaller size Au NPs in the Cu-TiO_2 samples. The Au NPs on the titania surface not only enhance the photocatalytic activity of titania but also act as active centers for sensing and other catalytic properties. This gives the insight that the cluster of 4-nm Au NPs can be easily impregnated onto some support using this facile single-step sol–gel method. EDX analysis is done to find the elemental composition of synthesized materials. Fig. 4 shows a typical EDX spectrum of Au/Cu-TiO_2 with 1 wt% copper and 0.5% gold in the titania matrix were estimated from EDX analysis.

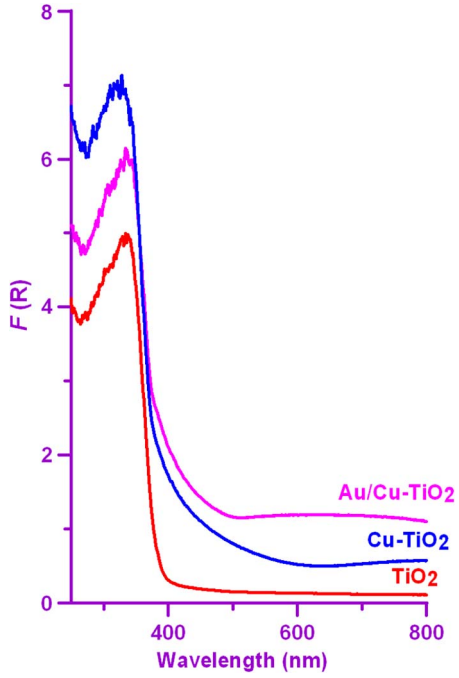

Fig. 5. Optical absorbance of TiO_2, Cu-TiO_2, and Au/Cu-TiO_2.

3.2. Optical Properties

The diffuse reflectance spectra of TiO_2, Cu-TiO_2, and Au/Cu-TiO_2 were taken, and the ordinate axis of these spectra is converted into a Kubelka–Munk function using the following equation:

$$F(R) = \frac{(1-R)^2}{2R}$$

where R is the reflectance [26]. The Kubelka–Munk function $F(R)$ is basically the absorbance, where the effects of scattering are eliminated. Fig. 5 shows the absorbance spectra of TiO_2, Cu-TiO_2, and Au/Cu-TiO_2, and in these spectra, we can notice a red shift in the absorption peak between TiO_2 and Cu-TiO_2, and this red shift could be attributed to the charge transfer transition between the metal ion d electrons and TiO_2 conduction or valance band. In the UV wavelength region (200–400 nm) of the spectrum, the relative intensities of the $F(R)$ show in a decreasing order for Cu-TiO_2, Au/Cu-TiO_2, and TiO_2. A similar trend was found in a recent report [25] that at lower copper doping into TiO_2 showed an enhanced absorption in the UV region, while at a higher concentration of copper on TiO_2 showed reduced UV absorption. In this paper, after gold modification, reduction in the UV absorption of Cu-TiO_2 could be explained because of surface coverage with gold NPs. However, in the visible wavelength region (450–800 nm), we can notice that after gold modification into Cu-TiO_2, the absorbance is considerably enhanced, and this enhanced absorbance could be due to the surface plasmon resonance originated from the collective oscillation of free electrons [14]. Au/Cu-TiO_2 shows an enhancement of the absorbance in the visible region (450–800 nm), and hence, this material is capable of working effectively with solar radiation for photocatalytic applications.

The PL spectrum gives the insight to study the efficiency of charge carrier trapping and the electron–hole recombination in the semiconductor. Fig. 6 depicts the PL spectra of TiO_2, Cu-TiO_2, and Au/Cu-TiO_2 with the excitation wavelength of 325 nm and the PL spectra. The broad PL spectra in Fig. 6 upon Gaussian curve fitting show two Gaussian peaks A and B with varying relative intensities between them. It is quite obvious from the arbitrary scales in the ordinate axes of these three spectra that peak A shows more variation in the PL intensity than Peak B. Moreover, the

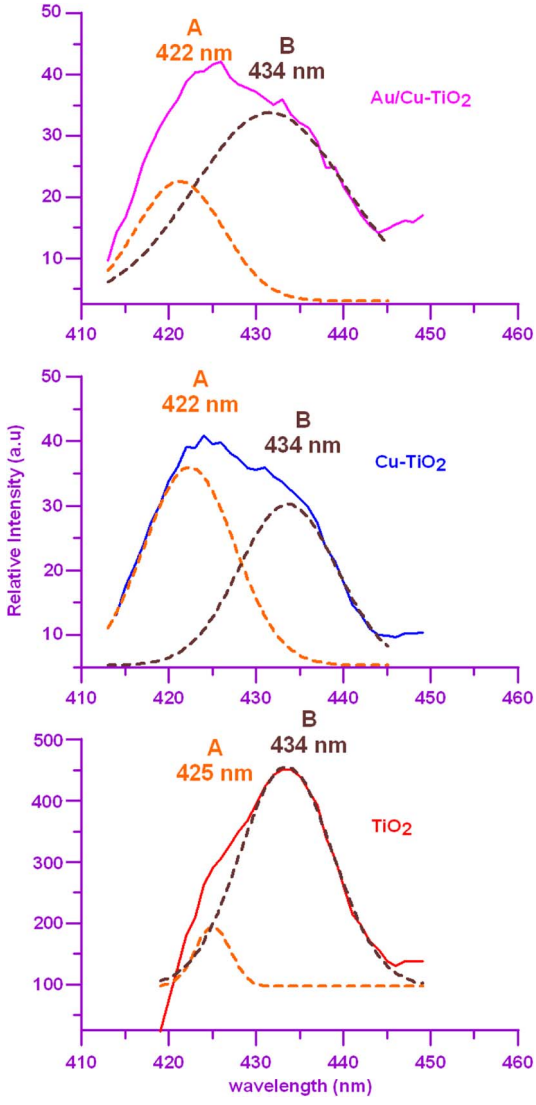

Fig. 6. PL spectra of TiO_2, Cu-TiO_2, and Au/Cu-TiO_2.

centers of peak B in the three spectra are at 434 nm, and they remain unchanged, whereas the center of peak A is at 425 nm for TiO_2, and for Cu-TiO_2 and Au/Cu-TiO_2, it is slightly blue shifted to 422 nm. Also, the overall PL intensities for Cu-TiO_2 and Au/Cu-TiO_2 decrease by a factor of 9 with respect to the overall PL intensity of TiO_2, and this could be attributed to the charge transfer between copper oxide and titania. Also, the higher PL intensity in the case of pure TiO_2 indicates the reduced electron–hole lifetime due to the rapid recombination; with copper doping, the electron–hole recombination process is slowed down. This indicates that the gold modification brings about the trapping of electrons because of Schottky barrier formation.

4. Conclusion

We synthesized Au/Cu-TiO_2 nanocomposites characterized by XRD, diffuse reflectance spectroscopy, PL, and TEM. The synthesized Au/Cu-TiO_2 shows enhanced absorption in the visible region (450–800 nm) compared with Cu-TiO_2 and TiO_2, and this makes this material capable of making use of solar radiation. Also, the PL intensity for Au/Cu-TiO_2 decreases, and this reduction in the PL signal could be attributed to the decrease in electron–hole recombination, which is a quality desired

for the enhancement of photocatalytic activity. Our present results show that Au/Cu-TiO_2 could be used as a photocatalyst workable in the visible spectrum of light, and also, it can be applied for fuel cells, gas sensing, and optical sensors.

References

[1] A. Fujishima and K. Honda, "Electrochemical photolysis of water at a semiconductor electrode," *Nature*, vol. 238, no. 5358, pp. 37–38, Jul. 1972.

[2] X. Chen and S. S. Mao, "Titanium dioxide nanomaterials: Synthesis, properties, modifications, and applications," *Chem. Rev.*, vol. 107, no. 7, pp. 2891–2959, Jul. 2007.

[3] I. H. Tseng, J. C. Wu, and H. Y. Chou, "Effects of sol–gel procedures on the photocatalysis of Cu/TiO_2 in CO_2 photoreduction," *J. Catal.*, vol. 221, no. 2, pp. 432–440, Jan. 2004.

[4] Y. Li, W.-N. Wang, Z. Zhan, M.-H. Woo, C.-Y. Wu, and P. Biswas, "Photocatalytic reduction of CO_2 with H_2O on mesoporous silica supported Cu/TiO_2 catalysts," *Appl Catal B*, vol. 100, no. 1/2, pp. 386–392, Oct. 2010.

[5] Y. H. Xu, D. H. Liang, M. L. Liu, and D. Z. Liu, "Preparation and characterization of Cu_2O-TiO_2 efficient photocatalytic degradation of methylene blue," *Mater. Res. Bull.*, vol. 43, no. 12, pp. 3474–3482, Dec. 2008.

[6] Y. Sakata, T. Yamamoto, T. Okazaki, H. Imamura, and S. Tsuchiya, "Generation of visible light response on the photocatalyst of a copper ion containing TiO_2," *Chem Lett.*, vol. 68, pp. 1253–1254, 1998.

[7] A. Teleki, N. Bjelobrk, and S. E. Pratsinis, "Flame-made Nb- and Cu-doped TiO_2 sensors for CO and ethanol," *Sens. Actuators B, Chem.*, vol. 130, no. 1, pp. 449–457, Mar. 2008.

[8] X.-H. Li, P. Zhu, G. Liu, J. Zhang, R. Song, Y.-K. Ee, P. Kumnorkaew, J. F. Gilchrist, and N. Tansu, "Light extraction efficiency enhancement of III-nitride light-emitting diodes by using 2-D close-packed TiO_2 microsphere arrays," *J. Display Technol.*, vol. 9, no. 5, pp. 324–332, May 2013.

[9] P. Zhu, G. Liu, J. Zhang, and N. Tansu, "FDTD analysis on extraction efficiency of GaN light-emitting diodes with microsphere arrays," *J. Display Technol.*, vol. 9, no. 5, pp. 317–323, May 2013.

[10] X. C. Jiang, T. Herricks, and Y. N. Xia, "Monodispersed spherical colloids of Titania: Synthesis, characterization, and crystallization," *Adv. Mater.*, vol. 15, no. 14, pp. 1205–1209, Jul. 2003.

[11] Y. K. Ee, P. Kumnorkaew, R. A. Arif, H. Tong, H. P. Zhao, J. F. Gilchrist, and N. Tansu, "Optimization of light extraction efficiency of III-Nitride light emitting diodes with self-assembled colloidal-based microlenses," *IEEE J. Sel. Top. Quantum Electron.*, vol. 15, no. 4, pp. 1218–1225, Jul./Aug. 2009.

[12] W. H. Koo, W. Youn, R. Song, L. Zhao, N. Tansu, and F. So, "Light extraction of organic light emitting diodes by defective hexagonal-close-packed array," *Adv. Funct. Mater.*, vol. 22, no. 16, pp. 3453–3459, Aug. 2012.

[13] X. Qiu, M. Miyauchi, K. Sunada, M. Minoshima, M. Liu, Y. Lu, D. Li, Y. Shimodaira, Y. Hosogi, Y. Kuroda, and K. Hashimoto, "Hybrid Cu_xO/TiO_2 nanocomposites as risk reduction materials in indoor environment," *ACS Nano*, vol. 6, no. 2, pp. 1609–1618, Feb. 2012.

[14] X. Z. Li and F. B. Li, "Study of Au/Au^{3+}-TiO_2 photocatalysts toward visible photooxidation for water and wastewater treatment," *Environ. Sci. Technol.*, vol. 35, no. 11, pp. 2381–2387, 2001.

[15] C. Y. Wang, C. Y. Liu, and J. Chen, "The surface chemistry of hybrid nanometer-sized particles I. Photochemical deposition of gold on ultrafine TiO_2 particles," *Colloid Surf. A*, vol. 131, no. 1–3, pp. 271–280, Jan. 1998.

[16] C. Burda, X. Chen, R. Narayanan, and A. El-Sayed, "Chemistry and properties of nanocrystals of different shapes," *Chem. Rev.*, vol. 105, no. 4, pp. 1025–1102, Apr. 2005.

[17] Z. Liu, W. Hou, P. Pavaskar, M. Aykol, and S. B. Cronin, "Plasmon resonant enhancement of photocatalytic water splitting under visible illumination," *Nano Lett.*, vol. 11, no. 3, pp. 1111–1116, Mar. 2011.

[18] P. Christopher, H. Xin, A. Marimuthu, and S. Linic, "Singular characteristics and unique chemical bond activation mechanisms of photocatalytic reactions on plasmonic nanostructures," *Nat. Mater.*, vol. 11, no. 12, pp. 1044–1050, Dec. 2012.

[19] C.-Y. Chen, J. R. D. Retamal, I.-W. Wu, D.-H. Lien, M.-W. Chen, Y. Ding, Y.-L. Chueh, C.-I. Wu, and J.-H. He, "Probing surface band bending of surface-engineered metal oxide nanowires," *ACS Nano*, vol. 6, no. 11, pp. 9366–9372, 2012.

[20] C.-Y. Chen, M.-W. Chen, J.-J. Ke, C.-A. Lin, J. R. D. Retamal, and J.-H. He, "Surface effects on optical and electrical properties of ZnO nanostructures," *Pure Appl. Chem.*, vol. 82, no. 11, pp. 2055–2073, 2010.

[21] M. W. Chen, J. R. D. Retamal, C. Y. Chen, and J. H. He, "Photocarrier relaxation behavior of a single ZnO nanowire UV photodetector: Effect of surface band bending," *IEEE Electron Device Lett.*, vol. 33, no. 3, pp. 411–413, Mar. 2012.

[22] M. W. Chen, C. Y. Chen, D. H. Lien, Y. Ding, and J. H. He, "Photoconductive enhancement of single ZnO nanowire through localized Schottky effects," *Opt. Exp.*, vol. 18, no. 14, pp. 14 836–14 841, Jul. 2010.

[23] J. H. He, P. H. Chang, C. Y. Chen, and K. T. Tsai, "Electrical and optoelectronic characterization of a ZnO nanowire contacted by focused-ion-beam-deposited Pt," *Nanotechnology*, vol. 20, no. 13, p. 135701, Apr. 2009.

[24] N. Lock, E. M. L. Jensen, J. Mi, A. Mamakhel, K. Norén, M. Qingbo, and B. B. Iversen, "Copper doped TiO_2 nanoparticles characterized by X-ray absorption spectroscopy, total scattering, and powder diffraction—A benchmark structure property study," *Dalton Trans.*, Apr. 15, 2013, DOI: 10.1039/C3DT00122A, to be published.

[25] A. G. Shtukenberg, Y. O. Punin, and O. I. Artamonova, "Effect of crystal composition and growth rate on sector zoning in solid solutions grown from aqueous solutions," *Mineralogical Mag.*, vol. 73, no. 3, pp. 385–398, Jun. 2009.

[26] J. Tauc, R. Grigorovici, and A. Vancu, "Optical properties and electronic structure of amorphous germanium," *Phys. Stat. Sol.*, vol. 15, no. 2, pp. 627–637, 1966.